PHYSICS AND CHEMISTRY OF SOLID STATE
V. 26, No. 4 (2025) pp. 718-732
Section: Physics

DOI: 10.15330/pcss.26.4.718-732

Vasyl Stefanyk Carpathian National University

ФІЗИКА І ХІМІЯ ТВЕРДОГО ТІЛА
Т. 26, № 4 (2025) С. 718-732
Фізико-математичні науки

UDC: 539.2

ISSN 1729-4428 (Print)
ISSN 2309-8589 (Online)

T.S. Kavetskyy[1,2,3], O.V. Zubrytska[1], O.I. Matskiv[1], M. Stievenard[4], O. Šauša[2,5], H. Švajdlenková[5,6], V.M. Soloviev[3,7], A.O. Bielinskyi[7,8], J. Ostrauskaite[9], A.E. Kiv[3,10]

Photopolymerization and photodegradation of polymers after long-term UV light exposure

[1]*Drohobych Ivan Franko State Pedagogical University, Drohobych, Ukraine, kavetskyy@yahoo.com;*
[2]*Institute of Physics, Slovak Academy of Sciences, Bratislava, Slovakia;*
[3]*South Ukrainian National Pedagogical University named after K.D. Ushynsky, Odesa, Ukraine, kiv.arnold20@gmail.com;*
[4]*Department of Chemistry, IUT de LILLE, Villeneuve d'Ascq, Lille, France;*
[5]*Department of Nuclear Chemistry, FNS, Comenius University, Bratislava, Slovakia;*
[6]*Polymer Institute, Slovak Academy of Sciences, Bratislava, Slovakia;*
[7]*Kryvyi Rih State Pedagogical University, Kryvyi Rih, Ukraine, vnsoloviev2016@gmail.com;*
[8]*Kyiv National Economic University named after Vadym Hetman, Kyiv, Ukraine;*
[9]*Kaunas University of Technology, Kaunas, Lithuania;*
[10]*Ben-Gurion University of the Negev, Beer-Sheva, Israel*

Over the past two decades, research into photostimulated processes in polymeric materials has gained new momentum, driven both by the growing demand for functional polymers with controllable properties and the need to understand their long-term stability under operational conditions. Current approaches combine the development of new materials, such as photopolymerization systems for 3D printing and biosensing, with a deep fundamental study of the mechanisms of photoinduced changes, including the role of free volume and the dynamics of molecular motions. UV light irradiation is known to affect materials, and possibly change their properties in certain conditions due to the existence of 'subthreshold radiation effects'. Polymerization reactions may also need light exposure to happen, this is photopolymerization, and UV light exposure is a very good way to start these reactions. However, UV light can degrade the polymer if it is exposed to it for a prolonged period of time. In this case, the newly formed polymer will undergo changes in its network structure, which can change its properties. A combination of positron annihilation lifetime spectroscopy (PALS), attenuated total reflectance Fourier transform infrared (ATR-FTIR) and electron paramagnetic resonance (EPR) spectroscopy in complementary with computer modeling using recurrence analysis, was used to obtain information on the network properties of polymer matrix based on acrylated epoxidized soybean oil (AESO) and vanillin dimethacrylate (VDM) with and without a photoinitiator (2,2-dimethoxy-2-phenylacetophenone) (DMPA) according to the proposed light on/off protocol in view of long-term UV light exposure.

Keywords: photopolymerization, photodegradation, UV light, irradiation, polymers, free volume, properties, photostructural changes, computer modeling, recurrence analysis.

Received 16 April 2025; Accepted 28 October 2025.

Introduction

Photopolymerization is a process in which the structure of monomers and oligomers changes after exposure to ultraviolet light. These structural changes lead to the strengthening of the material due to crosslinking. The advantages of this process are low energy consumption, high efficiency, low emissions of volatile organic compounds and wide practical applications as coatings, inks and adhesives, as well as in high-tech industries such as microelectronics, optoelectronics, laser imaging and nanotechnology. Structural changes associated with the formation of radicals and the transformation of double bonds are of great interest in the

process of photopolymerization.

The main goal of this work is the study of photopolymerization and photodegradation for the acrylated epoxidized soybean oil (AESO) and vanillin dimethacrylate (VDM) materials with or without a photoinitiator, 2,2-dimethoxy-2-phenylacetophenone (DMPA) (Fig. 1), which can be used as holding matrixes for biosensors [1-6] and biobased materials for 3D printing [7-13]. Knowledge of these processes is important from at least two perspectives: firstly, it is necessary to know the stability of the structure of these materials and the influence of UV radiation, and secondly, this research will increase the knowledge of these biopolymers' properties.

I. Experimental

1.1. Thermocouple temperature measurements.

The experiment on in-situ photopolymerization was controlled through thermocouple (TC). Temperature measurements during photopolymerization were carried out using a measurement system developed at the Institute of Physics of the Slovak Academy of Sciences [14]. T-type thermocouples (Omega Engineering) record the temperature every 1 second. The temperature measuring thermocouple had a measuring tip 4 mm away from the inner edge of the silicon chamber for positron annihilation lifetime spectroscopy (PALS) measurement and at half the height of the sample space. The geometry of the sample location was identical to the PALS measurement.

1.2. The photopolymerization apparatus.

The apparatus used for the photopolymerization is composed of a sample chamber, UV light, a set of 5 thermocouples used to monitor the temperature inside the sample and around it, and a photodetector probe used to measure the light intensity coming out of the sample for the duration of the experiment. All of this equipment is linked to a computer where different illumination protocols can be programmed, and the goal is to see how the data will change as the reaction occurs.

1.3. The sample chamber.

The chamber for this experiment is designed to have a final sample of 15 mm diameter and about 3.0 mm thickness. It is composed of: one silicone mold to contain the mixture with two very thin holes for the insertion of one or two thermocouples; two quartz glass panes (lets UV light go through), to close down the silicone mold (glass is used because it is easier to remove the sample from it afterwards); two aluminum disks with screws to seal the chamber. On the top side, there is a slit for the placement of the photodetector probe. The second option, for PALS experiments, is to cover the upper part of the chamber with a thin 8 μm Kapton foil sufficiently permeable to positrons.

1.4. Characterization techniques.

A combination of positron annihilation lifetime spectroscopy (PALS), attenuated total reflectance Fourier transform infrared (ATR-FTIR) and electron paramagnetic resonance (EPR) spectroscopy in complementary with computer modeling using complex network methods, was used to obtain information on the network properties of polymer matrix based on AESO:VDM with and without a photoinitiator (PI), DMPA, according to the proposed light on/off protocol in view of long-term UV light exposure. PALS is known as the most developed technique in positron annihilation spectroscopy – a useful method for microstructural analysis of complex macromolecular structure – for polymer applications [15, 16]. PALS is an uncommon technique used to study the behavior and properties of materials at the atomic and molecular scale focusing on the free volumes. It is based on the annihilation of positrons inside of materials and measures the lifetime of positrons or positronium (bound sate of an electron and a positron). The data produced by this type of analysis are the intensity and lifetime of separate components based on different annihilation processes, which can be used to determine further information about a sample, for example the size of the pores in this sample. This technique is non-destructive, but requires long periods of analysis in order to have good results.

PALS measurements were performed on a digital spectrometer with a resolution of about 320 ps (FWHM) based on a pair of scintillation detectors with BaF_2 crystals and a digital acquisition system based on the DRS4 V5 digitizer (PSI, Switzerland) and Q-PALS software [17, 18]. Measurement of the resolving function of the spectrometer and correction for annihilation in a positron source with an activity of approximately 2 MBq were performed using a defect-free Al standard. The spectra were evaluated using the LT program, Polymers version [19].

ATR-FTIR spectroscopy was used to study the cured polymers. The spectra were recorded in the wavenumber range 4000-600 cm^{-1}.

The EPR measurements of the samples were carried out on the Varian E4 spectrometer, X-band at constant frequency ~9.47 GHz to study the formation of free radicals in the cured polymers.

1.5. Illumination of samples.

Photopolymerization was done with UV LED light (365 nm). Another experiment was conducted to monitor changes in surface structure under the influence of long-term exposure to UV radiation.

The cured samples were irradiated using a UV light

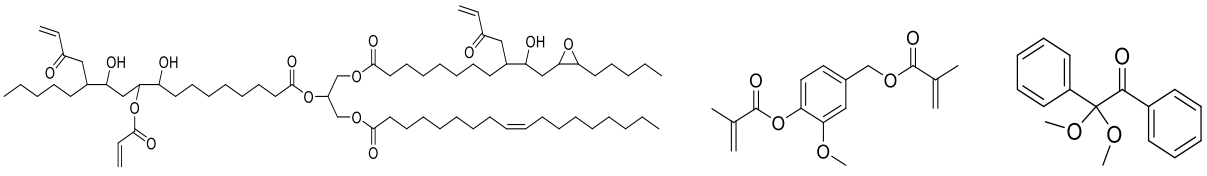

AESO **VDM** **DMPA**

Fig. 1. Chemical structure of the AESO, VDM and DMPA.

from high-pressure mercury-vapor lamp, both at the same time and in the same conditions. For each sample, two separate data acquisitions were made; one for the bottom part of the sample (directly in contact with the UV light during the photopolymerization and subsequently illuminated after curing) and one for the top part (opposite to the light). The flux density at the sample surface was 28.5 mW/cm^2.

II. Results and Discussion

The acrylated soybean oil-based AESO/VDM (without photoinitiator) and AESO/VDM/DMPA (with 3 mol% photoinitiator (PI) – DMPA) photocross-linked polymers with ratio of monomers AESO and VDM as 1:0.5 mol were polymerized and prepared by continuous and interrupted illumination protocol.

2.1. Continuous illumination with PI.

The continuous illumination protocol consists of long phases of illumination followed by long phases of dark, repeated several times with varying durations. It is divided in 3 different time periods following each other.

First time period – continuous illumination with PI from 0 to 60000 seconds:

The time dependency of sample temperature and light intensity after penetration of the sample for the first time period is plotted in Fig. 2.

There is a temperature jump that is characteristic of this type of exothermic reactions, but the most interesting part is the exponential growth of the intensity for the whole duration of the illumination.

With the zoom, we can see the small intensity jump at the start, but the curve immediately goes down as the reaction happens (Fig. 3).

Second time period – continuous illumination with PI from 60000 to 150000 seconds:

The time dependency of sample temperature and light intensity after penetration of the sample for the second time period is plotted in Fig. 4. The goal of this new irradiation parameters is to see how the intensity and temperature evolves after being submitted to a long dark period.

It is interesting to note that the intensity level instantly jumps back to the previous level when the light is switched back on, which shows some permanent changes in the sample caused by the prolonged UV exposition. Also, we can see that the trend of the first part is continuing during the illumination (on a smaller scale, Fig. 5).

Third time period – continuous illumination with PI from 150000 to 230000 seconds:

The time dependency of sample temperature and light intensity after penetration of the sample for the third time

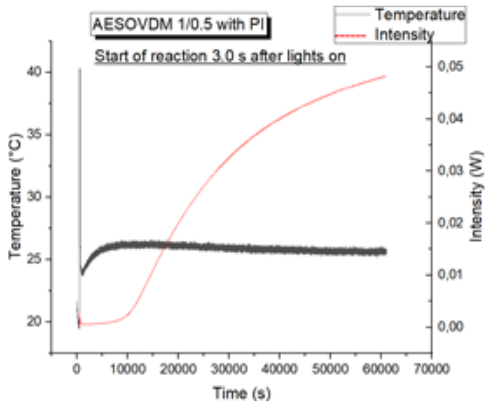

Fig. 2. Time dependency of sample temperature and light intensity after penetration of the sample AESO:VDM (1:0.5) with photoinitiator (PI) for the first time period.

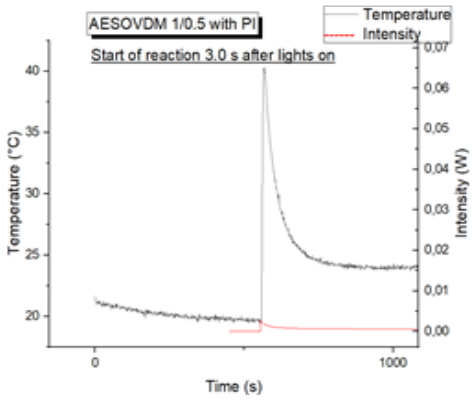

Fig. 3. Time dependency of sample temperature and light intensity after penetration of the sample AESO:VDM (1:0.5) with photoinitiator (PI) for the first time period zoomed on the beginning of reaction peak.

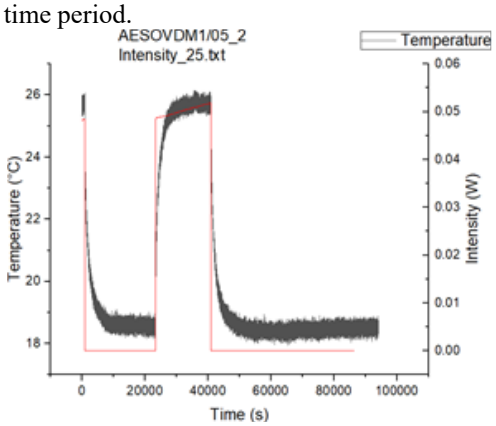

Fig. 4. Time dependency of sample temperature and light intensity (red curve) after penetration of the sample AESO:VDM (1:0.5) with photoinitiator (PI) for the second time period.

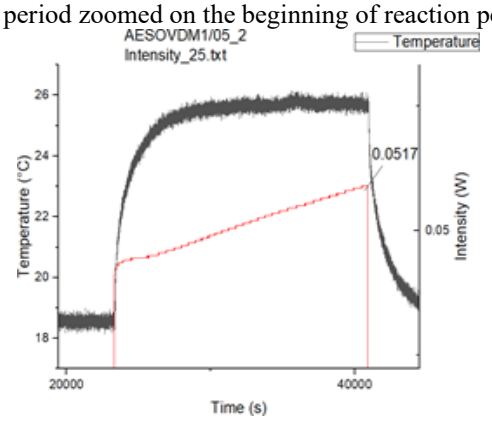

Fig. 5. Time dependency of sample temperature and light intensity (red curve) after penetration of the sample AESO:VDM (1:0.5) with photoinitiator (PI) for the second time period zoomed.

period is plotted in Fig. 6. The interest of this part is to confirm the fact that the intensity level is not affected by dark periods when the light is turned back on.

The interesting part is that the intensity immediately jumps back at 0.0517 W, which is the exact maximum value when the light was turned off in the previous part (see Fig. 7). In this experiment, we confirmed the fact that permanent changes are made inside of the sample whenever it is exposed to UV light for extended periods of time.

2.2. Continuous illumination without PI.

For this section, the protocol is the exact same as in the previous one, the only difference is the sample; now, it does not contain photoinitiator (PI).

The results are identical to the last part with higher values of intensity due to the lack of photoinitiator, so analyzing the graphics the same way has little interest. However, comparing the intensities for the first part reveals interesting results (Fig. 8).

The comparison of the two intensity curves on the same graph shows a major difference in shape of curve: the intensity immediately jumps to a high value when there is no photoinitiator, whereas it rises slowly when a photoinitiator is present. Also, there is a big difference between the intensity values: the red curve (without PI) reaches values two times higher than the blue curve (with PI). It could be explained as the photoinitiator absorbs the light, leading to lower transmitted intensity. As exposure continues, the PI is consumed, so absorption drops and the transmitted intensity slowly rises. Since, the transmitted intensity rapidly rises without photoinitiator which absorbs the light.

2.3. Interrupted illumination with PI.

The interrupted illumination protocol consists of very short (a few seconds) peaks of illumination followed by longer periods of dark. The illumination times are augmenting with each phase while the dark periods are reduced, with the final phase being a continuous illumination for several hours.

The principle of this method is the following: an illumination of a set duration happens, followed by a dark period of a longer duration, and this process is repeated 2 times with the same values; then, this process is repeated for a series of 5 different dark period durations (Table 1), and when this process is finished, it is started again with a different value of illumination time (Table 2). For example, according to the tables, we have this combination: A1 - A1 - A2 - A2 - A3 - A3 - A4 - A4 - A5 - A5 - B1 - B1 - B2 - ... - I5 - I5, and with at the end a continuous illumination for 22000 seconds.

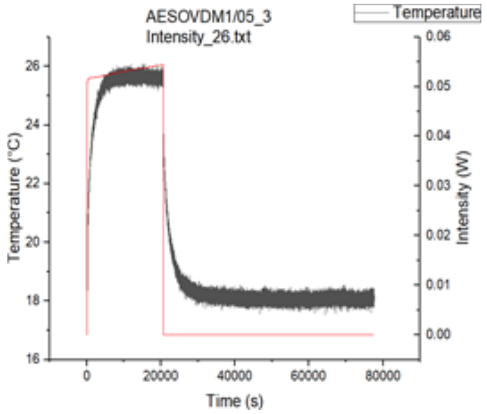

Fig. 6. Time dependency of sample temperature and light intensity (red curve) after penetration of the sample AESO:VDM (1:0.5) with photoinitiator (PI) for the third time period.

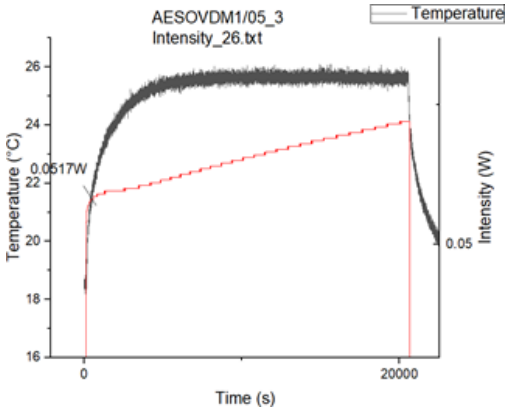

Fig. 7. Time dependency of sample temperature and light intensity (red curve) after penetration of the sample AESO:VDM (1:0.5) with photoinitiator (PI) for the third time period zoomed.

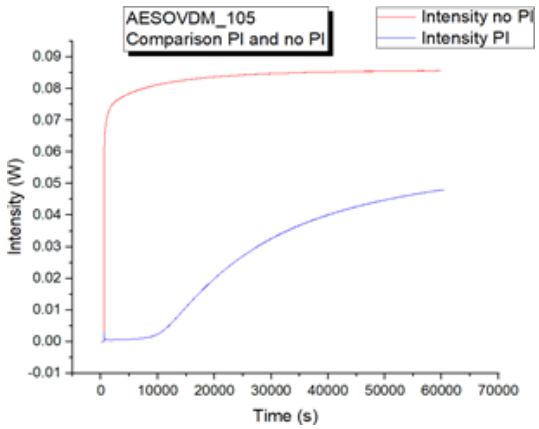

Fig. 8. Comparison of the time dependency of light intensity after penetration of the sample AESO:VDM (1:0.5) with (blue) and without (red) photoinitiator (PI).

Table 1.

Dark time values.

Protocol	1	2	3	4	5
Dark time (s)	60	120	180	240	300

Table 2.

Illumination time values.

Protocol	A	B	C	D	E	F	G	H	I
Illumination time (s)	1	10	20	30	40	50	100	200	1000

The principle of this protocol being explained, we can now analyze the figures produced with the data of this protocol. For the following graphics, the processes are grouped by pair (A – B; C –D; E – F; G – H; I – continuous).

First time period – interrupted illumination with PI (A1 – B5):

The time dependency of sample temperature and light intensity after penetration of the sample for the first time period with repeated illumination time for 1 s and 10 s is plotted in Fig. 9. As we can see, the pattern described above is respected. The interesting part of this graphic is the trend; due to short illumination periods, the intensity peaks to a high value, causing the reaction to happen, but this causes the next peak to be less intense because of the change of structure inside the material, which is repeated for the next peak, etc.

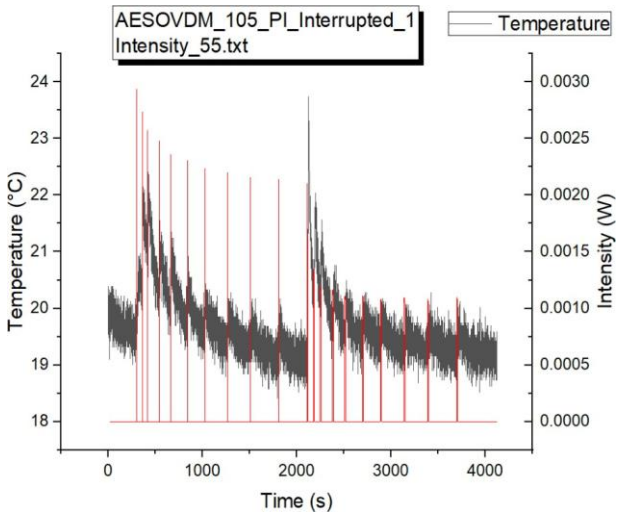

Fig. 9. Time dependency of sample temperature and light intensity (red curve) after penetration of the sample AESO:VDM (1:0.5) with photoinitiator (PI) for the first time period with repeated illumination time for 1 s (left part) and 10 s (right part).

Second time period – interrupted illumination with PI (C1 – D5):

The time dependency of sample temperature and light intensity after penetration of the sample for the second time period with repeated illumination time for 20 s and 30 s is plotted in Fig. 10.

The pattern is still the same with higher illumination durations. On this figure, we can see that the tendency to have a higher first peak is still present, but the trend is evolving during the duration of a cycle: we have a lowering intensity trend at the beginning, but it rises toward the end. This is due to the longer illumination periods allowing for the reaction within the sample to take place more effectively.

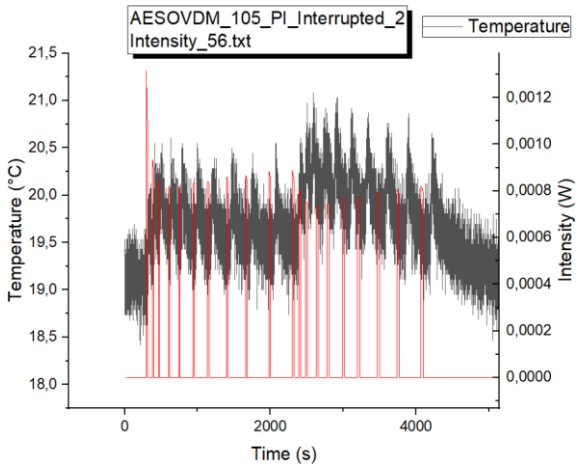

Fig. 10. Time dependency of sample temperature and light intensity (red curve) after penetration of the sample AESO:VDM (1:0.5) with photoinitiator (PI) for the second time period with repeated illumination time for 20 s (left part) and 30 s (right part).

Third time period – interrupted illumination with PI (E1 – F5):

The time dependency of sample temperature and light intensity after penetration of the sample for the third time period with repeated illumination time for 40 s and 50 s is plotted in Fig. 11. The trend started in the previous part continues, with the intensity level rising instead of dropping.

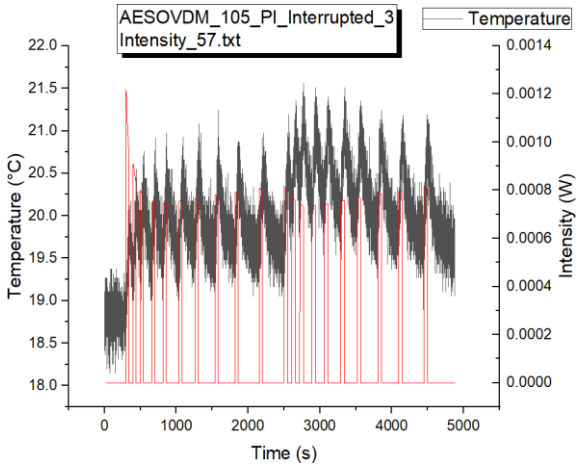

Fig. 11. Time dependency of sample temperature and light intensity (red curve) after penetration of the sample AESO:VDM (1:0.5) with photoinitiator (PI) for the third time period with repeated illumination time for 40 s (left part) and 50 s (right part).

Fourth time period – interrupted illumination with PI (G1 – H5):

The time dependency of sample temperature and light intensity after penetration of the sample for the fourth time period with repeated illumination time for 100 s and 200 s is plotted in Fig. 12. With this cycle, the illumination times are now longer than the dark times, which counters the effect of these dark periods and produces the trend of this figure, a slow rise of the intensity.

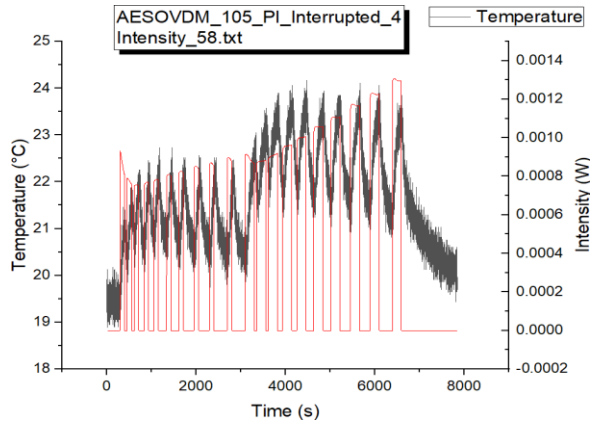

Fig. 12. Time dependency of sample temperature and light intensity (red curve) after penetration of the sample AESO:VDM (1:0.5) with photoinitiator (PI) for the fourth time period with repeated illumination time for 100 s (left part) and 200 s (right part).

Fifth time period – interrupted illumination with PI (I1 – continuous):

The time dependency of sample temperature and light intensity after penetration of the sample for the fifth time period with repeated illumination time for 1000 s and continuous illumination (22000 s) is plotted in Fig. 13.

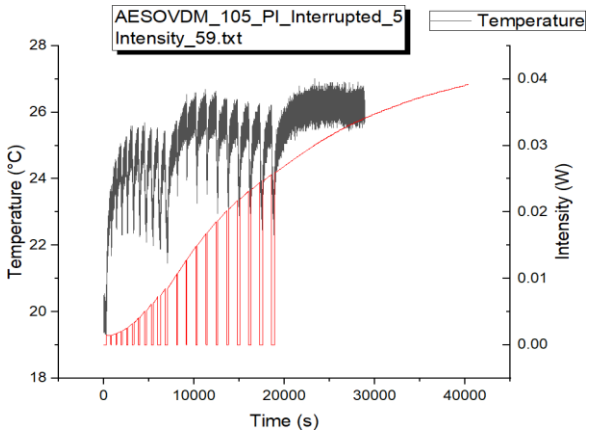

Fig. 13. Time dependency of sample temperature and light intensity (red curve) after penetration of the sample AESO:VDM (1:0.5) with photoinitiator (PI) for the fifth time period with repeated illumination time for 1000 s (left part) and continuous illumination (right part).

This figure concludes the experiment, with the trend now being a clear and progressive rise of the intensity. This trend is now very similar to the continuous illumination of the Fig. 2, due to the very long illumination times, which eventually even becomes continuous illumination (22000 s).

Summarizing the findings for the reaction system with PI, one may conclude the following.

• At the beginning:

The photoinitiator absorbs light strongly, reducing transmitted intensity. The most photons are used to generate radicals that start curing.

• As curing proceeds:

The photoinitiator molecules are consumed, so absorption decreases. The material becomes more transparent to the irradiation wavelength.

• Observation of increased intensity for the irradiated cured sample:

Because less light is absorbed, more light passes through → transmitted intensity increases, even though the sample is "cured".

The question is why the cured sample with PI still reduces UV light absorption with increasing illumination dose (so long or so slow to saturation level, see Fig. 8). In this case the definition of the time when the sample is "cured for practical use" is unclear.

2.4. Interrupted illumination without PI.

The protocol for this section is the same as for the previous part, the only difference being the composition of the sample, now without PI.

First time period – interrupted illumination without PI (A1 – B5):

The time dependency of sample temperature and light intensity after penetration of the sample for the first time period with repeated illumination time for 1 s and 10 s is plotted in Fig. 14.

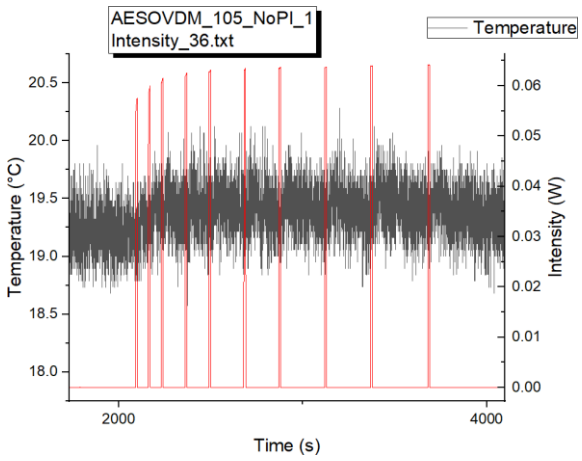

Fig. 14. Time dependency of sample temperature and light intensity (red curve) after penetration of the sample AESO:VDM (1:0.5) without photoinitiator (PI) for the first time period with repeated illumination time for 1 s (left part) and 10 s (right part).

Second time period – interrupted illumination without PI (C1 – D5):

The time dependency of sample temperature and light intensity after penetration of the sample for the second time period with repeated illumination time for 20 s and 30 s is plotted in Fig. 15.

Third time period – interrupted illumination without

PI (E1 – F5):

The time dependency of sample temperature and light intensity after penetration of the sample for the third time period with repeated illumination time for 40 s and 50 s is plotted in Fig. 16.

Fourth time period – interrupted illumination without PI (G1 – H5):

The time dependency of sample temperature and light intensity after penetration of the sample for the fourth time period with repeated illumination time for 100 s and 200 s is plotted in Fig. 17.

Fifth time period – interrupted illumination without PI (I1 – continuous):

The time dependency of sample temperature and light intensity after penetration of the sample for the third time period with repeated illumination time for 1000 s and continuous illumination (22000 s) is plotted in Fig. 18.

The trend in all these spectra (Figs. 14-18) is the same; a very slow increase in the intensity level as shown by a direct comparison of the intensity levels in Fig. 19. This figure is better to see the difference between the first step and the last one; this shows that the rise of intensity is very slow, but the levels are considerably higher than the sample with PI.

Thus, according to the continuous and interrupted illumination protocol applied, it is concluded that the cured sample containing photoinitiator exhibits higher light absorption than the cured sample without photoinitiator. This can be attributed to the more complete polymerization and slower consumption of PI, which intensively absorbs UV light, and gradually becomes incorporated into the network, while the sample without PI retains residual absorbing monomers and relatively quickly transits to a state with lower UV light absorption and, consequently, polymerization is less intensive.

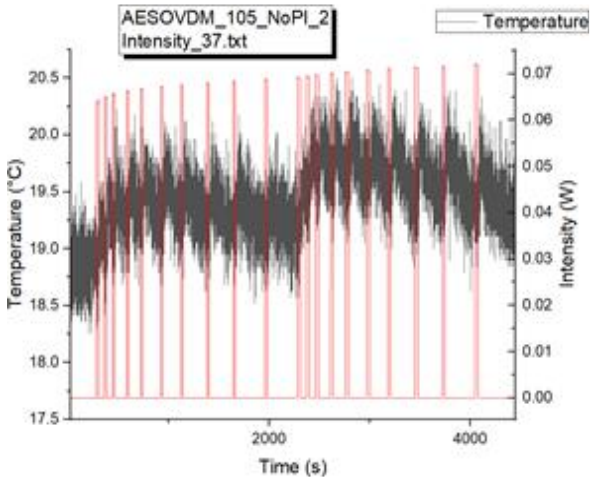

Fig. 15. Time dependency of sample temperature and light intensity (red curve) after penetration of the sample AESO:VDM (1:0.5) without photoinitiator (PI) for the second time period with repeated illumination time for 20 s (left part) and 30 s (right part).

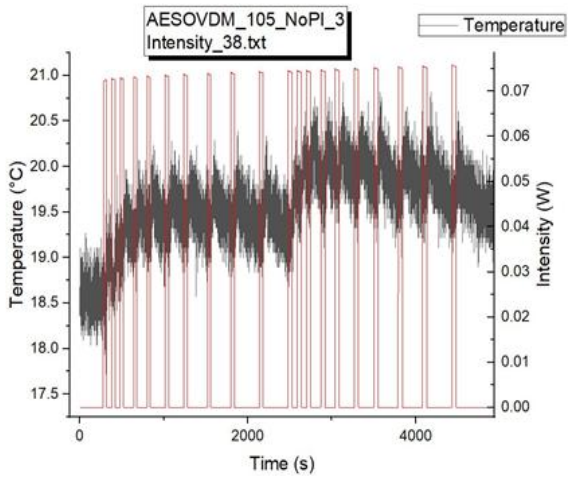

Fig. 16. Time dependency of sample temperature and light intensity (red curve) after penetration of the sample AESO:VDM (1:0.5) without photoinitiator (PI) for the third time period with repeated illumination time for 40 s (left part) and 50 s (right part).

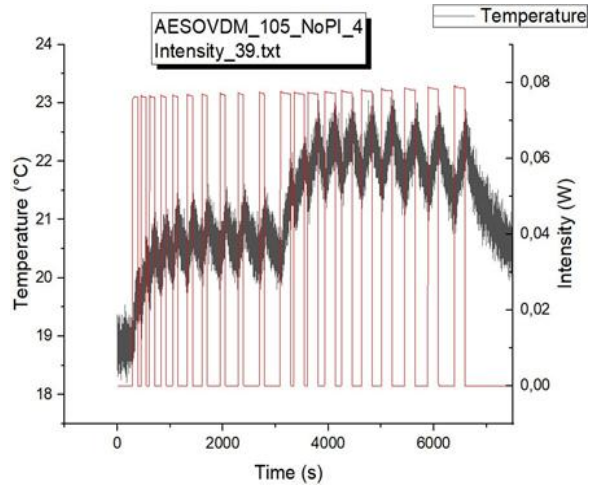

Fig. 17. Time dependency of sample temperature and light intensity (red curve) after penetration of the sample AESO:VDM (1:0.5) without photoinitiator (PI) for the fourth time period with repeated illumination time for 100 s (left part) and 200 s (right part).

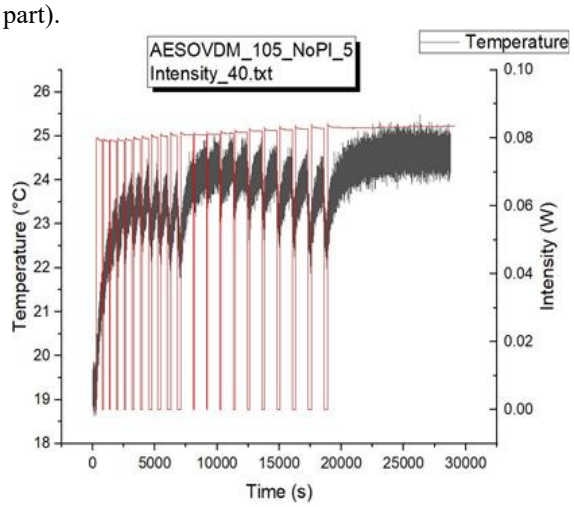

Fig. 18. Time dependency of sample temperature and light intensity (red curve) after penetration of the sample AESO:VDM (1:0.5) without photoinitiator (PI) for the fifth time period with repeated illumination time for 1000 s (left part) and continuous illumination (right part).

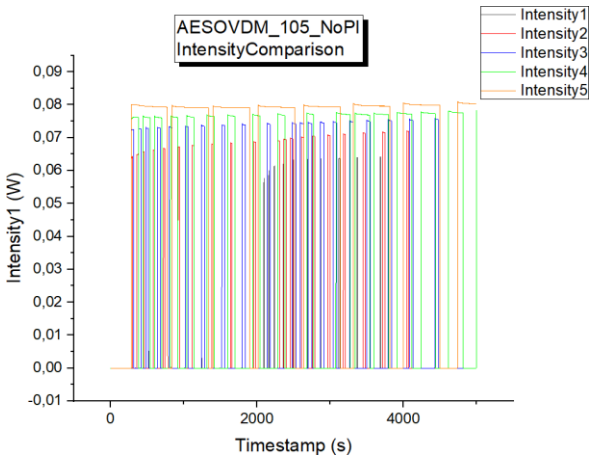

Fig. 19. Graphical comparison of the light intensity levels after penetration of the sample AESO:VDM (1:0.5) without photoinitiator (PI) during the examined 5 periods.

2.5. Analysis of the cured samples – post-curing stage.

The course of photopolymerization of AESO:VDM samples with and without a photoinitiator (PI) and different content of VDM was studied using PALS recently [20]. The crosslinking process was carried out under UV light, with and without PI. PALS was used to characterize the local free volume and its uniformity (Fig. 20). The results showed that an increased content of VDM containing aromatic rings led to a decrease in the local free volume in the cured polymer network [20, 21]. This in turn affected the diffusion properties of the polymer, especially in the case of water. Furthermore, an increase in the VDM content led to a decrease in the conversion of double bonds in the cured samples, as determined by near-infrared spectroscopy (NIR). This finding highlights a scenario in which the decrease in free volume is not necessarily related to an increase in the crosslink density of the polymer, but rather is a consequence of the occupation of part of the free space by aromatic rings in the polymer [20].

The goal of this subject being to determine the effects of long-term UV light exposure on the cured AESO:VDM (1:0.5) polymer (post-curing stage), the samples were submitted to different durations of exposure to UV light and analyzed by PALS and ATR-FTIR at the same protocol (Table 3). The samples were irradiated using a mercury UV light, both at the same time and in the same conditions. For each sample, two separate data acquisitions were made; one for the bottom part of the sample (directly in contact with the UV light during the photopolymerization) and one for the top part (opposite to the light).

The results obtained using PALS and ATR-FTIR for the cured samples during a continuous UV illumination are shown in Figs. 21 and 22, according to the time protocol used (Table 3). It is found via both techniques that the UV light exposure has an impact on the materials that are exposed to it during their photopolymerization or for irradiation to the formed samples. The changes can be rather significant for extended periods of irradiation to a material (increasing illumination dose), with an important transformation of its atomic or molecular properties (photo-induced structural changes).

At the same time, it is possible to see different sensitivities of the used techniques to surface changes of the investigated materials. While FTIR is sensitive to the increase of radiation dose from UV light on the side of the sample facing the light, because it is sensitive to changes in the surface area, PALS characterizes the properties of the sample volume, since the energy spectrum of positrons from the ^{22}Na source is continuous. Therefore, PALS lifetimes cannot capture changes in the thin layer on the sample surface and the dependence of lifetimes as well as

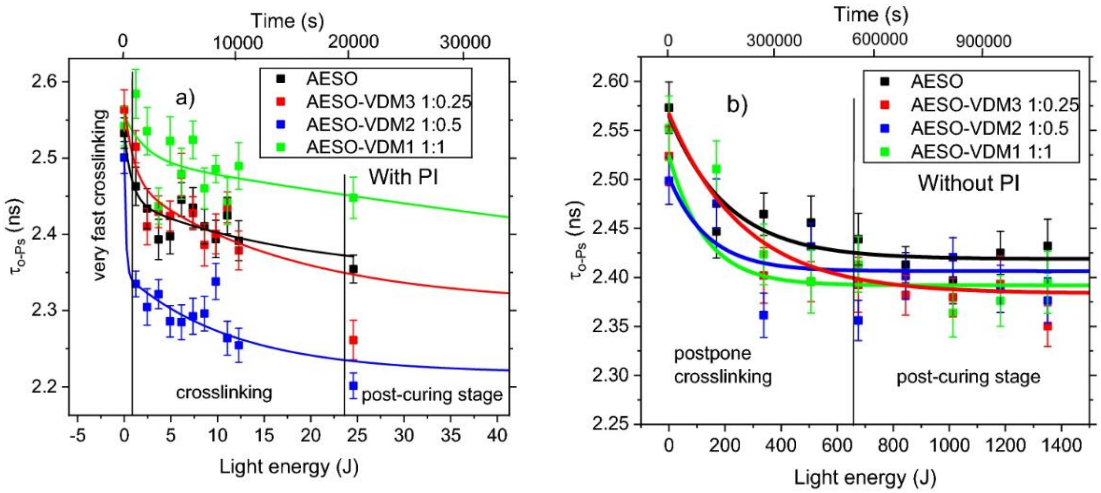

Fig. 20. The course of photopolymerization for the AESO:VDM samples with (a) and without (b) the photoinitiator (PI) studied with PALS. Total irradiation time as "Time" (top X-axis) and light energy absorbed in the sample volume as "Light energy" (bottom X-axis) are shown [20].

Table 3.

The illumination time protocol for the investigated AESO:VDM (1:0.5) samples.

Protocol	V1	V2	V3	V4	V5	V6
Irradiation period	5h16min	6h23min	9h06min	18h46min	26h42min	48h04min
Total irradiation time	5h16min	11h39min	20h45min	39h21min	66h03min	114h07min

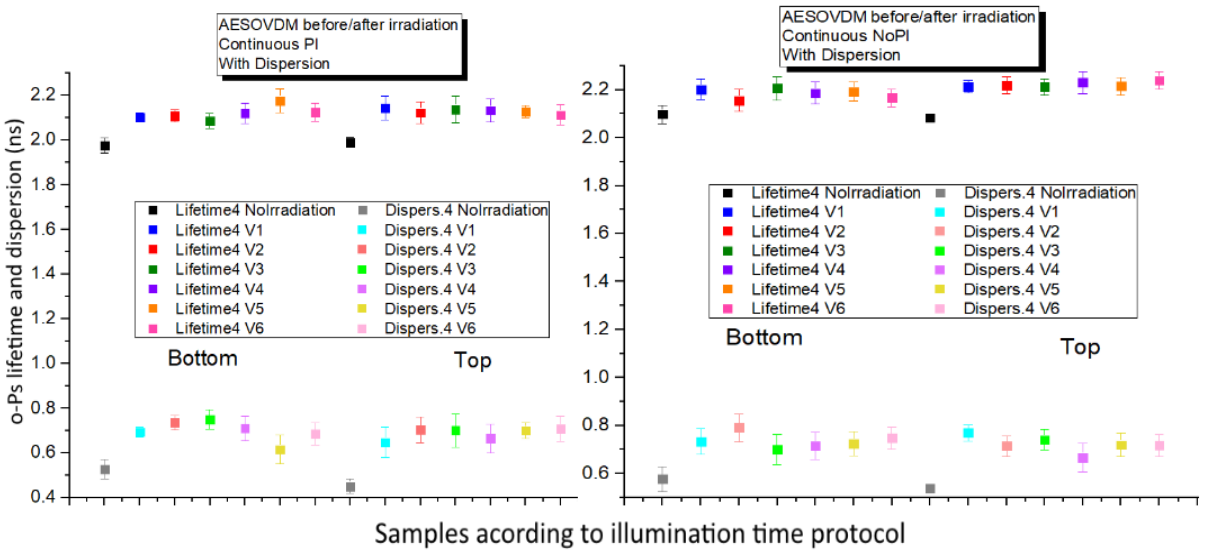

Fig. 21. PALS results (o-Ps lifetime and o-Ps lifetime dispersion) according to illumination time protocol for the cured samples AESO:VDM (1:0.5) with (left) and without (right) photoinitiator (PI) during a continuous UV illumination.

dispersion is practically constant with dose. An exception is the beginning of the UV lamp irradiation process, where, probably under the influence of intense UV light, changes in the local free volume (enlargement) have already occurred throughout the sample volume and also a broadening of the size distribution of these local free volumes. This is shown by an increase in the dispersion of the lifetimes analyzed using the LT program in the continuous lifetime mode. This may indicate degradation processes.

Analyzing the surface changes with ATR-FTIR during a continuous UV illumination, there are a few noticeable peaks in the recorded spectra (Fig. 22): the 1180-1200 cm^{-1} (C–O–C), 1700-1750 cm^{-1} (C=O), 2700-2900 cm^{-1} (C–H), and 3500-3600 cm^{-1} (O–H) peaks (Table 4) [22]. In the case of the sample with PI, directly in contact with the UV light during the photopolymerization "bottom" (Fig. 22a), the peaks represent the O–H and C=O groups inside of the sample increase with each irradiation period, while the peaks represent the C–H and C–O–C groups decrease. It could be due to the photo-structural changes inside the polymer matrix within the existence of subthreshold radiation effects in polymers, leading to the observed changes in the intensity of IR bands and photodegradation. It is interesting that in the case of the sample with PI, opposite to the light "top" (Fig. 22b), such effect was not observed.

On the other hand, in the case of the sample without PI, directly in contact with the UV light during the photopolymerization "bottom" (Fig. 22c), such changes in the intensity of IR bands are even more pronounced comparing with the sample with PI (Fig. 22a). This suggests less crosslinked (cured) structure. At the same time, the effect is slightly observed in the case of the sample without PI, opposite to the light "top" (Fig. 22d), showing a preferential increase the intensity of O–H groups inside of the sample with each irradiation period.

The appearance and increase in the intensity of the bands of carbonyl C=O (1700-1750 cm^{-1}) groups has also been found under study of the gamma-ray irradiation-induced oxidation of polyethylene and other polymers [23, 24], that is direct evidence of oxidative degradation.

Thus, our finding could be also interpreted as photo-induced oxidative degradation in the framework of the main principals of the subthreshold radiation effects in polymers, and such oxidative degradation is controllable, i.e., may be reduced or enhanced using a photoinitiator or without it.

The results obtained using EPR spectroscopy for the cured samples during UV illumination and dark periods are shown in Fig. 23. The graduate decrease in concentration of free radicals during dark periods of 3 and 6 minutes was observed. That is, in dark, the radical population decreases over time.

Thus, the EPR results show that irradiation leads to maximum radical generation due to photoinitiator activation, whereas in the absence of light, the radicals gradually decay through polymerization and termination reactions, resulting in a decreased radical concentration.

2.6. Computer modeling – recurrence analysis.

Polymer materials and processes often exhibit complex, nonlinear behavior, from curing reactions to mechanical degradation. Traditional linear analysis can miss subtle dynamic patterns in these systems. Recurrence analysis is a nonlinear time-series analysis approach well-suited to detecting such patterns. It relies on recurrence plots (RPs) – graphical representations of times at which a system's state repeats or is similar to a past state [25, 26]. By visualizing recurrences in a system's phase space trajectory, RPs can reveal hidden regularities, chaos, or regime shifts in polymer-related data [26-28]. This method is particularly valuable for polymers, where phenomena like curing, aging, or damage evolution may produce complex signals. Researchers often quantify RPs using Recurrence Quantification Analysis (RQA), which provides measures like:

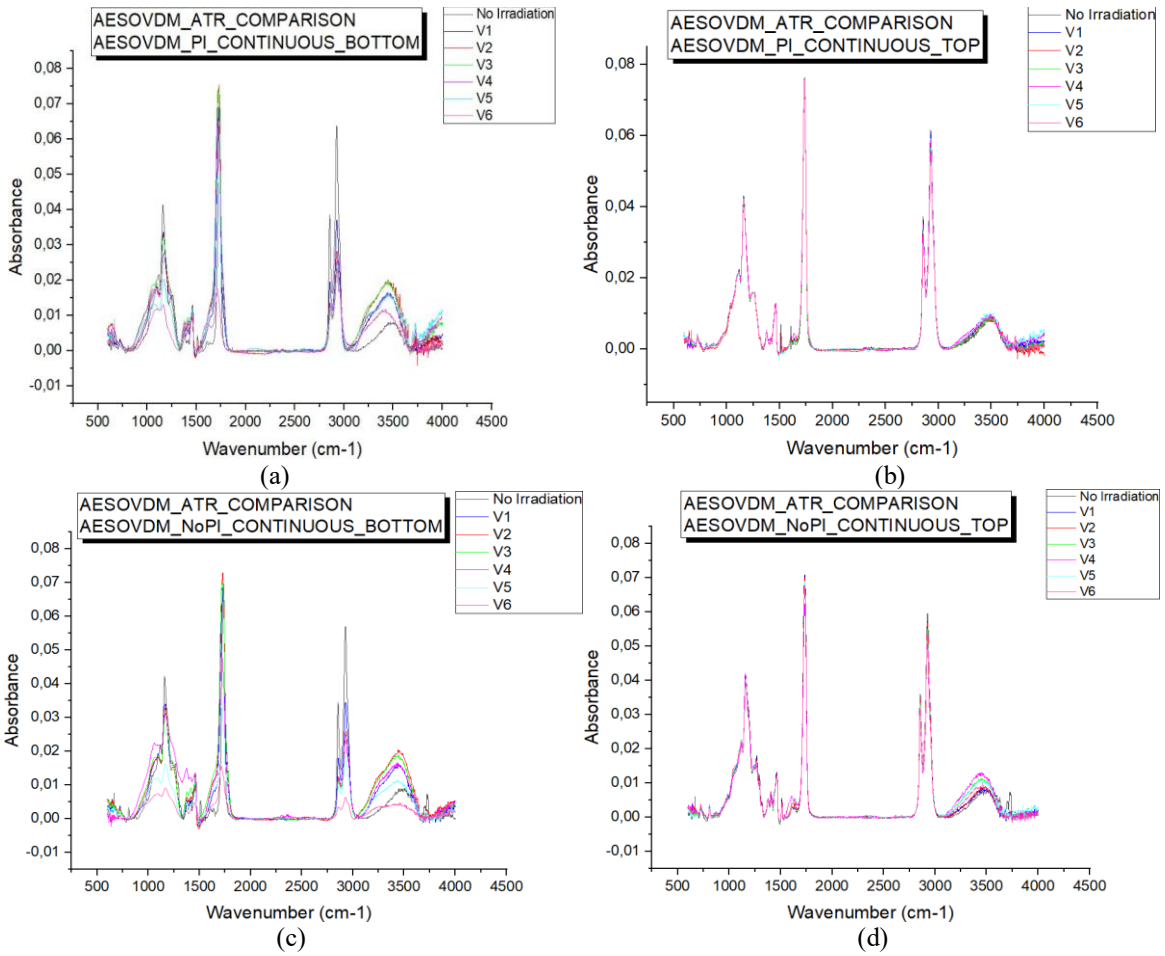

Fig. 22. ATR-FTIR results for the cured samples AESO:VDM (1:0.5) with (a – directly in contact with the UV light during the photopolymerization "bottom", b – opposite to the light "top") and without (c – directly in contact with the UV light during the photopolymerization "bottom", d – opposite to the light "top") photoinitiator (PI) during a continuous UV illumination.

Table 4.

Assignments of the main IR bands [22].

Major functional group	Absorption frequency region			
O–H	3650-3540			
N–H	3500-3300	1650-1590	900-650	
=CH–H	3100-3070	1420-1410	900-880	
=C–H	3100-3000	2000-1600		
C–H	2900-2700	1440-1320	680-610	630
$-CH_3$	2880-2860	2970-2950	1470-1430	1380-1370
O–H	2700-2500	1410-1310	1350-1260	720-590
C≡C	2260-2100	2140-2100		
C=O	1750-1700			
C=C	1680-1620	1600-1500		
C–C	1350-1000			
C–N	1340-1250			
C–O–C	1200-1180			
–C–H	770-730			

Determinism (*DET*). Determinism quantifies the fraction of recurrence points that form diagonal lines of at least some length ℓ_{min} [26, 27]. In other words, it is the percentage of recurrences that are part of sequential time segments where the trajectory remains close over ℓ_{min} or more consecutive steps. A higher *DET* (near 100%) means most recurrence points are aligned on diagonal segments, indicating that whenever a state recurs, it continues to evolve in parallel with the nearby orbit for some time – a signature of deterministic predictability. Conversely, a low *DET* (with many isolated single-point recurrences) suggests more stochastic or unpredictable behavior. For example, uncorrelated noise produces an RP dominated by solitary points (very few diagonal lines, hence low *DET*), whereas a deterministic chaotic system yields many extended diagonals (high *DET*).

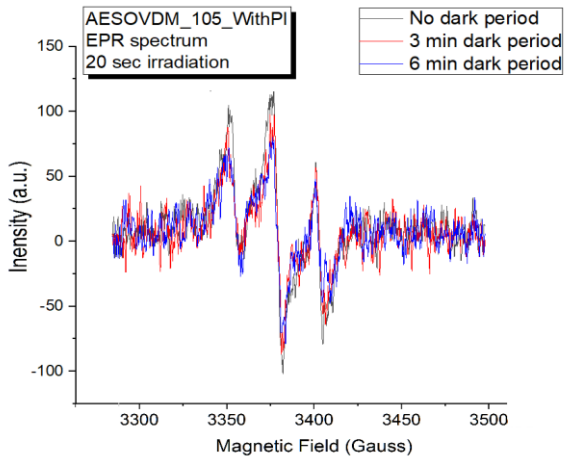

Fig. 23. EPR results for the cured samples AESO:VDM (1:0.5) with photoinitiator (PI) during UV illumination and dark periods.

Shannon Entropy of Diagonal Lines (*DLEn*). This measure evaluates the complexity of the diagonal line length distribution.

One computes $p(\ell) = P(\ell)/\sum_{l=l_{min}}^{N} P(\ell)$ as the probability distribution of a diagonal line having length ℓ, and then calculates the Shannon entropy regarding this probability [26, 27]. A higher entropy indicates a broader spread of diagonal lengths (more complexity in the temporal recurrence structure), whereas a low entropy suggests that diagonal lines are mostly of similar length or that only very short diagonals occur. In effect, $DLEn$ captures the richness of deterministic structure in the dynamics – for example, a purely periodic system might have low entropy (most recurrences occur at a fixed period, yielding similar line lengths), while a chaotic system with multiple time scales of recurrence would have a higher entropy of line lengths.

Together, RPs and RQA metrics allow researchers to characterize polymer system behavior beyond what simple averages or Fourier analysis can show. In the following sections, we review how recurrence analysis has been applied to polymers – spanning experimental studies of material degradation, defect detection in composites, and polymerization processes – highlighting insights gained from these nonlinear techniques.

In our recentrecent study, the curing of AESO:VDM was examined using multifractal detrended fluctuation analysis [1]. While strictly speaking this is not recurrence analysis, multifractal analysis also demonstrated the identification of recurring dynamic patterns: each time the UV light was switched on or off, the system's temperature fluctuations showed an abrupt increase in "complexity" or multifractality, which can be interpreted as the system entering a new state. The recurrence plot concept can be applied here by considering the state vector as recent temperature readings; an increase in recurrent complexity at light on/off suggests a qualitative change – hypothesized as a quasi-phase transition related to polymer network formation. This indicates that even in polymerization kinetics, recurrence or complexity analyses can reveal critical moments (like initiation or termination of polymer growth) that might correspond to structural self-organization events.

Our complementary analysis [29] of the same AESO:VDM system under the light on/off protocol recasts the temperature time series as visibility graphs [30] and tracks their evolution in a sliding window, showing that illumination toggles reorganize the signal's network geometry in step with cure stage transitions. At lamp turn-on, the normalized Laplacian's algebraic connectivity rises sharply and higher spectral moments spike, indicating a rapid gain in global connectivity and triadic closure within the visibility network; as the system approaches gelation and enters quasi-steady segments, these spectral indicators plateau before surging again at subsequent toggles. In parallel, topological metrics such as maximum degree, closeness, harmonic and betweenness centralities peak at the same instants, revealing hub-like time points and "bridge" instants that concentrate shortest paths when the kinetics reorganize. Read through the lens of recurrence plots, these network transients correspond to the appearance of longer, more coherent diagonal families during organized ramps, followed by enhanced vertical structure (laminarity and trapping) in mobility-limited intervals; the successive spikes in spectral gap and natural connectivity mirror the temporary formation of tightly knit subdynamics that a time-resolved RQA would register as synchronized recurrence episodes. Because the network indicators respond reproducibly across cycles and formulations, they provide a scale-free corroboration of the recurrence-based regime map: initiation bursts, auto-acceleration, gelation/vitrification dwell, and post-cure relaxations are all marked by coordinated changes in both graph spectra and RP textures. Notably, the complex-network results dovetail with independent probes (PALS/NIR/EPR) of microstructural evolution and radical population, strengthening the physical interpretation that the observed geometric reorganizations are not merely variance shifts but genuine state-space transitions of the curing polymer.

Fig. 24 illustrates the comparative dynamics of temperature fluctuations, measured from the photopolymerization process with PI and measures of DET and $DLEn$.

In Fig. 24 (a) the temperature record shows repeated light ON/OFF cycles, while sliding-window DET measures how consistently short segments repeat (diagonal structure in the RP). DET jumps to ~1 whenever the window straddles a switching edge, where the signal follows a near-monotonic ramp – rapid heating after ON or directed cooling after OFF – so many segment pairs evolve almost identically and form long diagonals. As the window moves onto the illuminated or dark plateaus, the ramp contribution fades, small heterogeneous fluctuations dominate, and DET falls to a low baseline.

Mechanistically, ON activates the photoinitiator, producing a radical burst and gel-effect auto-acceleration; OFF stops radical generation and the network relaxes along a repeatable cooling path. Plateaus are shaped by initiator depletion, oxygen clean-up (early), diffusion-limited termination, and growing crosslink density, which fragment diagonal lines and depress DET. It captures how similar local paths are. Peak timing and width mark the initiation/auto-acceleration and quench/relaxation windows, while the suppressed baseline reflects the progressive loss of short-horizon predictability as the

network densities.

Fig. 24 (b) presents the dynamics of $DLEn$ – the Shannon entropy of diagonal-lengths in a sliding-window recurrence plot. It reflects the spread of predictability times: a broad mix of diagonal lengths (many shadowing durations) gives high entropy; nearly periodic/laminar motion or dynamics broken into short, noisy pieces yields a narrow distribution and low entropy.

In the data, entropy spikes at every switch and relaxes to a low baseline on the illuminated and dark plateaus. At light ON, activation of the photoinitiator triggers a radical burst and gel-effect auto-acceleration; a window straddling this onset captures a mix of a steep heating ramp, early relaxation, and nascent microfluctuations. The coexistence of long and short diagonals broadens the distribution, inflating entropy. As the system settles on the illuminated plateau, initiator depletion and diffusion-limited termination tame the kinetics; fluctuations become small and uniform, diagonals shorten and homogenize, and entropy collapses.

When the light is turned OFF, radical production ceases and the network undergoes multi-timescale thermal/structural relaxation. The window again blends rapid quench, viscoelastic cooling, and approach to the dark plateau, widening the diagonal-length distribution and lifting entropy before it decays to a laminar baseline. The largest peak at the first onset reflects a mobile matrix and the strongest exotherm; later cycles, constrained by higher conversion and viscosity, produce narrower, lower peaks.

Taken together, these results establish recurrence analysis as a compact, physics-aware diagnostic for polymers. In aging dielectrics, it quantifies the migration from coherent, repetitive conduction to sporadic, bursty regimes that presage failure. In composites, it enhances ultrasonic and process monitoring by converting subtle waveform instabilities into robust, interpretable indices for detecting and sizing defects, and for tuning operating conditions. In polymerization, and especially in photopolymerization, it illuminates stage transitions and coupled thermo-chemical events and offers a pathway to closed-loop quality control in advanced manufacturing. Because the method characterizes geometry in state space rather than relying on long stationary records or specific models, it adapts readily across materials, sensors, and processing routes. As polymer research and production become increasingly data-rich, recurrence plots and their quantifiers provide a unifying vocabulary for recognizing defects, instabilities, and regime changes early – precisely when intervention is most effective.

2.7. Mechanisms of photopolymerization and photodegradation of polymers.

Polymers are materials with a wide variety of atomic configurations in the same sample. Chemical bonds are also characterized by diversity. Single, double and other chemical bonds can be in a variety of excited states, which is usually not taken into account when interpreting experimental results.

Structural transformations in polymers occur as a result of electron-lattice interactions. The energy of electronic excitations is transferred to the lattice, causing the corresponding structural rearrangements. Free radicals play the main role in these processes. This is explained by their high mobility and wide energy spectrum. Therefore, in practice, various methods are used to obtain a large concentration of free radicals.

First, a photoinitiator is used, which is a supplier of free radicals. Next, to break chemical bonds, the polymer is irradiated with subthreshold radiation, namely ultraviolet (UV), which affects only the electronic subsystem. The UV energy is selected to break the corresponding bonds and form free radicals. In the steady state, the rate of free radical creation is equal to the rate of their reduction as a result of polymerization.

When interpreting the kinetics of interrupted irradiation, it is necessary to take into account that when UV irradiation is turned off, the concentration of free

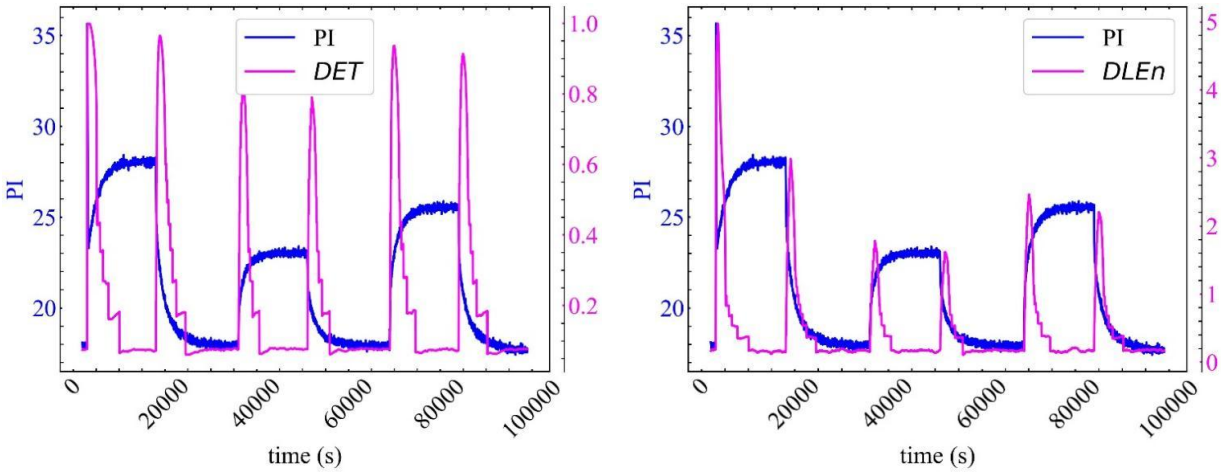

(a) (b)

Fig. 24. Photopolymerization under periodic illumination: thermocouple temperature (blue) and sliding-window RQA metrics. (a) Determinism (DET) and (b) diagonal-line entropy ($DLEn$) computed with sliding window $= 2000$ s, step $= 25$ s, embedding dimension $d_E = 1$, time delay $\tau = 1$, and $\varepsilon = 0.1$. DET rises to ≈1 when the window straddles ON/OFF edges (coherent heating/cooling ramps) and drops on illuminated/dark plateaus; $DLEn$ peaks at the same edges (broad distribution of diagonal lengths, i.e., diverse predictability times) and collapses on plateaus – together pinpointing initiation/auto-acceleration and quench/relaxation transitions.

radicals in the sample drops sharply, which affects the polymerization rate. When UV is turned on again, the polymerization kinetics are affected by radiation-stimulated diffusion of free radicals, just as they were when it was initially turned on. Radiation-stimulated diffusion is due to the uneven distribution of free radicals over the thickness of the sample.

Ultimately, when complete polymerization (hardening) occurs, the effect of UV is reduced to the destruction (degradation) of the polymer that has arisen. Now new chemical bonds are excited and destroyed, and subthreshold mechanisms of radiation defect formation are turned on.

Conclusions

A combination of PALS, ATR-FTIR, and EPR spectroscopy techniques with computer modeling using recurrence analysis, was used to obtain information on the photopolymerization and photodegradation of polymers after long-term UV light exposure for acrylated epoxidized soybean oil (AESO) and vanillin dimethacrylate (VDM) with and without a photoinitiator according to the proposed light on/off protocol. Photocross-linked polymers based on AESO:VDM were selected due to their potential application in biotechnology and biosensing, in particular for the creation of highly sensitive electrochemical biosensors. The PALS, ATR-FTIR, and EPR studies showed structural changes in AESO:VDM (1:0.5) investigated during continuous UV irradiation.

In the framework of Recurrence Quantification Analysis (RQA), focusing on determinism (*DET*) and diagonal-line entropy (*DLEn*) alone, the photopolymerization signal resolves into two clear behaviors. At each light ON/OFF, *DET* surges toward unity, showing that the trajectory follows a coherent, near-monotonic ramp; simultaneously *DLEn* spikes, indicating a broad mix of predictability times as the window captures both the directed front and the early stages of relaxation.

Since RQA measures are model-free and operate in short windows, they are robust to non-stationarity and provide a compact, physics-aware diagnostic for stage detection, segmentation, and comparative evaluation across formulations/illumination protocols. The recurrence-based regime map aligns with independent probes (PALS/ATR-FTIR/EPR) and complementary complex-network indicators, strengthening the interpretation that ON/OFF toggles drive quasi-phase-transition-like reorganizations of the polymer network. Overall, recurrence analysis turns raw temperature traces into actionable kinetic markers – pinpointing initiation and quench, tracking predictability and complexity, and enabling closed-loop monitoring of photopolymerization quality.

Finally, it has been established that when UV-radiation is applied to photocross-linked polymer materials, photopolymerization processes are accompanied by photodegradation ones. Possible mechanisms of photopolymerization and photodegradation of polymers are proposed.

Acknowledgments

This work was supported in part by the Ministry of Education and Science of Ukraine (projects Nos. 0122U000850, 0122U000874, 0122U001694, 0125U001054, 0125U002005, and 0125U002033), National Research Foundation of Ukraine (project No. 2020.02/0100), Slovak Grant Agency VEGA (projects Nos. 2/0166/22 and 2/0131/25), and Slovak Research and Development Agency (project No. APVV-21-0335). T.S.K. also acknowledges the SAIA (Slovak Academic Information Agency) for scholarship in the Institute of Physics of the Slovak Academy of Sciences in the framework of the National Scholarship Programme of the Slovak Republic. M.S. also acknowledges the Comenius University, Slovak Academy of Sciences and University of Lille for the internship within the Erasmus+ mobility project. This work has also received funding through the MSCA4Ukraine project (grant No. 1128327), which is funded by the European Union, and the EURIZON project (grant EU-3022), which is funded by the European Union (EURIZON H2020 project) under grant agreement No. 871072.

Kavetskyy T.S. – PhD in Physics and Mathematics, Associate Professor;
Zubrytska O.V. – PhD student;
Matskiv O.I. – PhD student;
Stievenard M. – MSc student;
Šauša O. – PhD in Physics;
Švajdlenková H. – PhD in Chemistry;
Soloviev V.M. – D.Sc. in Physics and Mathematics, Professor;
Bielinskyi A.O. – PhD student;
Ostrauskaite J. – PhD in Physical Sciences, Chemistry, Professor;
Kiv A.E. – D.Sc. in Physics and Mathematics, Professor.

[1] A.E. Kiv, V.N. Soloviev, A.O. Bielinskyi, M.A. Slusarenko, T.S. Kavetskyy, O. Šauša, H. Švajdlenková, I.I. Donchev, N.K. Hoivanovych, L.I. Pankiv, O.V. Nykolaishyn, O.R. Mushynska, O.V. Zubrytska, A.V. Tuzhykov, M. Kushniyazova, *Multifractal signatures of light-driven self-organization in acrylated epoxidized soybean oil polymers*, Semiconductor Physics, Quantum Electronics & Optoelectronics, 27(3), 366 (2024); https://doi.org/10.15407/spqeo27.03.366.

[2] T. Kavetskyy, O. Smutok, M. Goździuk-Gontarz, B. Zgardzińska, Y. Kukhazh, K. Zubrytska, N. Hoivanovych, O. Šauša, O. Demkiv, N. Stasyuk, M. Gonchar, J. Ostrauskaite, A. Kiv, E. Katz, *Impact of chemical composition of soybean oil and vanillin-based photocross-linked polymers on parameters of electrochemical biosensors*, Microchemical Journal, 201, 110618 (2024); https://doi.org/10.1016/j.microc.2024.110618.

[3] M. Goździuk, B. Zgardzińska, T. Kavetskyy, *Research on the sorption properties of biopolymer matrix based on soybean oil for the construction of biosensors to detect xenobiotics*, Acta Physica Polonica B Proceedings Supplement, 15, 4-A5 (2022); https://doi.org/10.5506/APhysPolBSupp.15.4-A5.
[4] M. Goździuk, T. Kavetskyy, D. Massana Roquero, O. Smutok, M. Gonchar, D.P. Královič, H. Švajdlenková, O. Šauša, P. Kalinay, H. Nosrati, M. Lebedevaite, S. Grauzeliene, J. Ostrauskaite, A. Kiv, B. Zgardzińska, *UV-cured green polymers for biosensorics: correlation of operational parameters of highly sensitive biosensors with nano-volumes and adsorption properties*, Materials, 15, 6607 (2022); https://doi.org/10.3390/ma15196607.
[5] M. Goździuk, B. Zgardzińska, T. Kavetskyy, K. Zubrytska, O. Smutok, O. Šauša, M. Lebedevaite, J. Ostrauskaite, A. Kiv, *Nanostructure research and amperometric testing to determine the detection capabilities of biopolymer matrices based on acrylated epoxidized soybean oil*, Acta Physica Polonica A, 139(4), 432 (2021); https://doi.org/10.12693/APhysPolA.139.432.
[6] T. Kavetskyy, Y. Kukhazh, K. Zubrytska, O. Smutok, O. Demkiv, M. Gonchar, O. Šauša, H. Švajdlenková, S. Kasetaite, J. Ostrauskaite, V. Boev, V. Ilcheva, T. Petkova, *Controlling the network properties of polymer matrices for improvement of amperometric enzyme biosensors: contribution of positron annihilation*, Acta Physica Polonica A, 137(2), 246 (2020); https://doi.org/10.12693/APhysPolA.137.246.
[7] C. Mendes-Felipe, I. Isusi, O. Gómez-Jiménez-Aberasturi, S. Prieto-Fernandez, L. Ruiz-Rubio, M. Marco Sangermano, J.L. Vilas-Vilela, *One-step method for direct acrylation of vegetable oils: A biobased material for 3D printing*, Polymers, 15, 3136 (2023); https://doi.org/10.3390/polym15143136.
[8] S. Grauzeliene, A.-S. Schuller, C. Delaite, J. Ostrauskaite, *Biobased vitrimer synthesized from 2-hydroxy-3-phenoxypropyl acrylate, tetrahydrofurfuryl methacrylate and acrylated epoxidized soybean oil for digital light processing 3D printing*, European Polymer Journal, 198, 112424 (2023); https://doi.org/10.1016/j.eurpolymj.2023.112424.
[9] S. Grauzeliene, B. Kazlauskaite, E. Skliutas, M. Malinauskas, J. Ostrauskaite, *Photocuring and digital light processing 3D printing of vitrimer composed of 2-hydroxy-2-phenoxypropyl acrylate and acrylated epoxidized soybean oil*, Express Polymer Letters, 17(1), 54 (2023); https://doi.org/10.3144/expresspolymlett.2023.5.
[10] M. Lebedevaite, V. Talacka, J. Ostrauskaite, *High biorenewable content acrylate photocurable resins for DLP 3D printing*, Journal of Applied Polymer Science, 138, e50233 (2021); https://doi.org/10.1002/app.50233.
[11] M. Lebedevaite, J. Ostrauskaite, *Influence of photoinitiator and temperature on photocross-linking kinetics of acrylated epoxidized soybean oil and properties of the resulting polymers*, Industrial Crops & Products, 161, 113210 (2021); https://doi.org/10.1016/j.indcrop.2020.113210.
[12] A. Navaruckiene, E. Skliutas, S. Kasetaite, S. Rekštytė, V. Raudoniene, D. Bridziuviene, M. Malinauskas, J. Ostrauskaite, *Vanillin acrylate-based resins for optical 3D printing*, Polymers, 12, 397 (2020); https://doi.org/10.3390/polym12020397.
[13] M. Lebedevaite, J. Ostrauskaite, E. Skliutas, M. Malinauskas, *Photoinitiator free resins composed of plant-derived monomers for the optical μ-3D printing of thermosets*, Polymers, 11, 116 (2019); https://doi.org/10.3390/polym11010116.
[14] H. Švajdlenková, A. Kleinová, O. Šauša, J. Rusnák, T.A. Dung, T. Koch, P. Knaack, *Microstructural study of epoxy-based thermosets prepared by "classical" and cationic frontal polymerization*, RSC Advances, 10, 41098 (2020); https://doi.org/10.1039/D0RA08298H.
[15] R.A. Pethrick, *Positron annihilation – A probe for nanoscale voids and free volume?*, Progress in Polymer Science, 22, 1 (1997); https://doi.org/10.1016/S0079-6700(96)00023-8.
[16] T. Goworek, *Positronium as a probe of small free volumes in crystals, polymers and porous media*, Annales Universitatis Mariae Curie-Sklodowska, Lublin – Polonia, 69, 1 (2014); https://doi.org/10.2478/umcschem-2013-0012.
[17] M. Petriska, S. Sojak, V. Slugeň, *Positron lifetime setup based on DRS4 evaluation board*, Journal of Physics: Conference Series, 505, 012044 (2014); https://doi.org/10.1088/1742-6596/505/1/012044.
[18] M. Petriska, S. Sojak, V. Kršjak, V. Slugeň, *Digital triple coincidence positron lifetime setup with DRS4 and its benefits*, AIP Conference Proceedings, 2411, 080009 (2021); https://doi.org/10.1063/5.0067492.
[19] J. Kansy, *Microcomputer program for analysis of positron annihilation lifetime spectra*, Nuclear Instruments and Methods in Physics Research Section A, 374, 235 (1996); https://doi.org/10.1016/0168-9002(96)00075-7.
[20] D.P. Královič, K. Cifraničová, H. Švajdlenková, D. Tóthová, O. Šauša, P. Kalinay, T. Kavetskyy, J. Ostrauskaite, O. Smutok, M. Gonchar, V. Soloviev, A. Kiv, *Effect of aromatic rings in AESO-VDM biopolymers on the local free volume and diffusion properties of polymer matrix*, Journal of Polymers and the Environment, 32, 2336 (2024); https://doi.org/10.1007/s10924-023-03097-1.
[21] D.P. Královič, K. Cifraničová, O. Šauša, H. Švajdlenková, T. Kavetskyy, A. Kiv. *The process of photopolymerization of acrylated soybean oil-based epoxides investigated by positron annihilation lifetime spectroscopy*, Chemical Papers, 77, 7257 (2023); https://doi.org/10.1007/s11696-022-02607-0.
[22] J. Coates, *Interpretation of Infrared Spectra, A Practical Approach*, in Encyclopedia of Analytical Chemistry, John Wiley & Sons, Ltd, pp. 1-23 (2006); https://doi.org/10.1002/9780470027318.a5606.
[23] H.-E. Shim, B.-M. Lee, D.-H. Lim, Y.-R. Nam, H.-J. Gwon, *A comparative study of gamma-ray irradiation-induced oxidation: polyethylene, poly (vinylidene fluoride), and polytetrafluoroethylene*, Polymers, 14, 4570 (2022); https://doi.org/10.3390/polym14214570.

[24] S. Liu, Q. Li, J. Wang, M. Lu, W. Zhang, K. Wang, W. Liu, M. Wang, *Study on the post-irradiation oxidation of polyethylenes using EPR and FTIR technique*, Polymer Degradation and Stability, 196, 109846 (2022); https://doi.org/10.1016/j.polymdegradstab.2022.109846.
[25] J.-P. Eckmann, S.O. Kamphorst, D. Ruelle, *Recurrence plots of dynamical systems*, Europhysics Letters, 4(9), 973 (1987); https://doi.org/10.1209/0295-5075/4/9/004.
[26] N. Marwan, M.C. Romano, M. Thiel, J. Kurths, *Recurrence plots for the analysis of complex systems*, Physics Reports, *438*(5–6), 237 (2007); https://doi.org/10.1016/j.physrep.2006.11.001.
[27] C.L. Webber, Jr., J.P. Zbilut, *Dynamical assessment of physiological systems and states using recurrence plot strategies*, Journal of Applied Physiology, 76(2), 965 (1994); https://doi.org/10.1152/jappl.1994.76.2.965.
[28] L.L. Trulla, A. Giuliani, J.P. Zbilut, C.L. Webber, Jr., *Recurrence quantification analysis of the logistic equation with transients*, Physics Letters A, 223(4), 255 (1996); https://doi.org/10.1016/S0375-9601(96)00741-4.
[29] A. Kiv, A. Bryukhanov, V. Soloviev, A. Bielinskyi, T. Kavetskyy, D. Dyachok, I. Donchev, V. Lukashin, *Complex network methods for plastic deformation dynamics in metals*, Dynamics, 3(1), 34 (2023); https://doi.org/10.3390/dynamics3010004.
[30] T. Kavetskyy, O. Zubrytska, M. Stievenard, O. Šauša, H. Švajdlenková, V. Soloviev, A. Bielinskyi, J. Ostrauskaite, A. Kiv, *Complex network methods, PALS, ATR-FTIR and EPR study of photopolymerization*, In: P. Petkov, M.E. Achour, C. Popov (Eds.), Nanotechnological Advances in Environmental, Cyber and CBRN Security. NATO Science for Peace and Security Series B: Physics and Biophysics. Springer, Dordrecht, Chap. 19, 265 (2025); https://doi.org/10.1007/978-94-024-2316-7_19.

Т.С. Кавецький[1,2,3], О.В. Зубрицька[1], О.І. Мацьків[1], М. Стівенард[4], О. Шауша[2,5], Х. Швайдленкова[5,6], В.М. Соловйов[3,7], А.О. Бєлінський[7,8], Й. Остраускайте[9], А.Ю. Ків[3,10]

Фотополімеризація та фотодеградація полімерів після тривалого впливу ультрафіолетового світла

[1]Дрогобицький державний педагогічний університет імені Івана Франка, Дрогобич, Україна, kavetskyy@yahoo.com;
[2]Інститут фізики Словацької академії наук, Братислава, Словаччина;
[3]Південноукраїнський національний педагогічний університет імені К.Д. Ушинського, Одеса, Україна, kiv.arnold20@gmail.com;
[4]Кафедра хімії, IUT de LILLE, Villeneuve d'Ascq, Лілль, Франція;
[5]Кафедра ядерної хімії, ФПН, Університет Коменського, Братислава, Словаччина;
[6]Інститут полімерів, Словацька академія наук, Братислава, Словаччина;
[7]Криворізький державний педагогічний університет, м. Кривий Ріг, Україна, vnsoloviev2016@gmail.com;
[8]Київський національний економічний університет імені Вадима Гетьмана, Київ, Україна;
[9]Каунаський технологічний університет, Каунас, Литва;
[10]Негевський університет Бен-Гуріона, Беер-Шева, Ізраїль

Протягом останніх двох десятиліть дослідження фотостимульованих процесів у полімерних матеріалах набули нового імпульсу, зумовленого як зростаючим попитом на функціональні полімери з контрольованими властивостями, так і необхідністю розуміння їхньої довгострокової стабільності в експлуатаційних умовах. Сучасні підходи поєднують розробку нових матеріалів, таких як системи фотополімеризації для 3D-друку та біосенсорики, з глибоким фундаментальним вивченням механізмів фотоіндукованих змін, включаючи роль вільного об'єму та динаміку молекулярних рухів. Відомо, що опромінення ультрафіолетовим світлом впливає на матеріали та, можливо, змінює їхні властивості за певних умов через існування «підпорогових радіаційних ефектів». Реакції полімеризації також можуть потребувати впливу світла, це фотополімеризація, і вплив ультрафіолетового світла є дуже хорошим способом для запуску цих реакцій. Однак ультрафіолетове світло може руйнувати полімер, якщо він піддається йому протягом тривалого періоду часу. У цьому випадку новоутворений полімер зазнає змін у своїй сітчастій структурі, що може змінити його властивості. Для отримання інформації про властивості сітки полімерної матриці на основі акрилованої епоксидованої соєвої олії (AESO) та ваніліндиметакрилату (VDM) з фотоініціатором (2,2-диметокси-2-фенілацетофенон) (DMPA) та без нього, згідно із запропонованим протоколом вмикання/вимикання світла з урахуванням тривалого впливу ультрафіолетового опромінення, було використано комбінацію позитронної анігіляційної спектроскопії часу життя (PALS), інфрачервоної спектроскопії з перетворенням Фур'є з ослабленим повним відбиттям (ATR-FTIR) та електронного парамагнітного резонансу (EPR) у доповненні з комп'ютерним моделюванням за використання рекурентного аналізу.

Ключові слова: фотополімеризація, фотодеградація, ультрафіолетове світло, опромінення, полімери, вільний об'єм, властивості, фотоструктурні зміни, комп'ютерне моделювання, рекурентний аналіз.